

# Polarization-entangled twin-photon ellipsometry

Kimani C. Toussaint, Jr.<sup>a</sup>, Ayman F. Abouraddy<sup>a</sup>, Matthew T. Corbo<sup>a</sup>,  
Alexander V. Sergienko<sup>a,b</sup>, Bahaa E. A. Saleh<sup>a</sup>, and Malvin C. Teich<sup>a,b</sup>

<sup>a</sup>Quantum Imaging Laboratory, Department of Electrical & Computer Engineering  
Boston University, Boston, MA, USA 02215-2421

<sup>b</sup>Department of Physics, Boston University, Boston, MA, USA 02215-2421

## ABSTRACT

The high accuracy required in traditional ellipsometric measurements necessitates the absolute calibration of both the source and the detector. We demonstrate that these requirements can be circumvented by using a non-classical source of light, namely, a twin-photon polarization-entangled source that produces type-II spontaneous parametric down-conversion, in conjunction with a novel polarization interferometer and coincidence-counting detection scheme. Our scheme exhibits two features that obviate the requirements of a calibrated source and detector. The first is the twin-photon nature of the source; we are guaranteed, on the detection of a photon in one of the arms of the setup, that its twin will be in the other, effectively serving as calibration of the source. The second is that the polarization entanglement of the source serves as an interferometer, thereby alleviating the need for calibrating the detector. The net result is that absolute ellipsometric data from a sample may be obtained. We present preliminary experimental results showing how the technique operates.

**Keywords:** Ellipsometry, quantum optics, nonlinear optics, polarization entanglement

## 1. INTRODUCTION

As the dimensions of the components used for integrated circuits decrease, the thicknesses of the isolating layers used for gate isolation, for example, need to also decrease.<sup>1</sup> Ellipsometric techniques are employed for non-destructive measurements of the film thicknesses used for these isolating layers. The accuracy of these measurements is very important for process control. Ellipsometry<sup>2-7</sup> is a well-established metrological technique that is used, particularly in the semiconductor industry, to determine the thickness and optical constants of thin-film samples. The sample is characterized by two parameters:  $\psi$  and  $\Delta$ . The quantity  $\psi$  is related to the magnitude of the ratio of the sample's eigenpolarization complex reflection coefficients,  $\tilde{r}_1$  and  $\tilde{r}_2$ , via  $\tan \psi = |\tilde{r}_1/\tilde{r}_2|$ ;  $\Delta$  is the phase shift between them.<sup>3</sup> The high accuracy required in traditional ellipsometric measurements necessitates the absolute calibration of both the source and the detector.

Ellipsometry makes use of a myriad of experimental techniques developed to circumvent the imperfections of the devices involved. The most common techniques are null and interferometric ellipsometry. However, both techniques suffer the drawback of requiring a reference sample for calibration prior to inserting the sample of interest.

In the traditional null ellipsometer,<sup>3</sup> depicted in Fig. 1, the sample is illuminated with a beam of light that can be prepared in any state of polarization. The reflected light, which is generally elliptically polarized, is then analyzed. The polarization of the incident beam is adjusted to compensate for the change in the relative amplitude and phase, introduced by the sample, between the two eigenpolarizations, so that the resulting reflected beam is linearly polarized. If passed through an orthogonal linear polarizer, this linearly polarized beam will yield a null (zero) measurement at the optical detector. The null ellipsometer does not require a calibrated detector since it does not measure intensity, but instead records a null. The principal drawback of

---

Further author information: (Send correspondence to A.V.S.)

A.V.S.: E-mail: alexsrg@bu.edu, Telephone: 1 617 353 6564, <http://www.bu.edu/qil>

Address: Boston University, Electrical & Computer Engineering Department, 8 Saint Mary's Street, Boston, MA, USA 02215-2421

null measurement techniques is the need for a reference to calibrate the null, for example to find its initial location (the rotational axis of reference at which an initial null is obtained) and then to compare this with the subsequent location upon inserting the sample into the apparatus. Such a technique thus alleviates the problem of an unreliable source and detector, but necessitates the use of a reference sample. The accuracy and reliability of all measurements depend on our knowledge of the parameters of this reference sample. In this case, the measurements are a function of  $\psi$ ,  $\Delta$ , and the parameters of the reference sample.

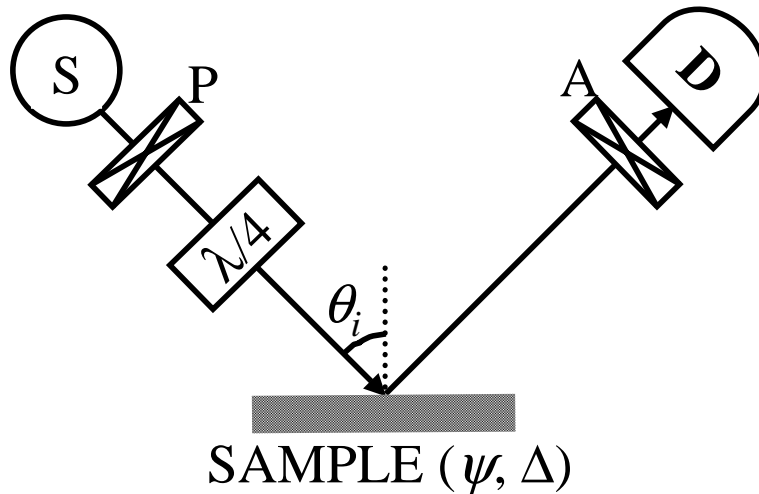


**Figure 1.** The null ellipsometer. S is an optical source, P a linear polarizer,  $\frac{\lambda}{4}$  a quarter-wave plate (compensator), A a linear polarization analyzer, and D an optical detector;  $\theta_i$  is the angle of incidence. The sample is characterized by the ellipsometric parameters  $\psi$  and  $\Delta$  defined in the text.

Another possibility is to perform ellipsometry that employs an interferometric configuration in which the light from the source follows more than one path, usually created via beam splitters, before reaching the detector. The sample is placed in one of those paths. We can then estimate the efficiency of the detector (assuming a reliable source) by performing measurements when the sample is removed from the interferometer. This configuration thus alleviates the problem of an unreliable detector, but depends on the reliability of the source and suffers from the drawback of requiring several optical components (beam splitters, mirrors, etc.). The ellipsometric measurements are a function of  $\psi$ ,  $\Delta$ , source intensity, and the parameters of the optical elements. The accuracy of the measurements are therefore limited by our knowledge of the parameters characterizing these optical components. This necessitates the use of a reference sample. The stability of the optical arrangement is also of importance to the performance of such a device.

Standard reference materials (SRMs), such as thermal oxide on silicon, offered by the National Institute of Standards & Technology (NIST), yield certified values of  $\Delta$  and  $\psi$  for specific angles of incidence (AI) and at a specific wavelength (usually 632.8 nm). This means that for any other AI, or wavelength used, reliable values of  $\Delta$  and  $\psi$  cannot be provided. Furthermore, even at the specified AI and wavelength,  $\psi$  and  $\Delta$  are only as accurate as the technique used to determine them, which invariably will rely on the use of some alternate reference. Recently, some work has been carried out on manufacturing reference materials for which  $\psi$  is an insensitive parameter around a specific AI.<sup>8</sup> Although these new reference materials promise some improvement over the older ones, the ellipsometric parameters are still not certified over the entire range of AIs.

It is worth mentioning that the certification data provided with SRMs are based on the assumption that one has a fully working ellipsometer without any errors. In other words, NIST guarantees that as long as one

has well-characterized polarizers and optical components, the exact wavelength of choice, and the exact AI of interest, then the SRM will yield the expected values of  $\psi$  and  $\Delta$ . Of course, a major problem is that one cannot decouple errors arising from the ellipsometer used with errors from the SRM.

Another issue of concern with SRMs is that their utility begins to erode when used outside their specified tolerances. For example, SRMs that are semiconductors become oxidized with time and thus must be viewed as three-phase (ambient–thin film–substrate) rather than two-phase systems. Some of these oxides have been shown to exhibit small variations in thickness over the entire wafer, which, of course, leads to errors in the model used. A surface whose properties change with time cannot be considered self-verifiable and thus cannot be used as a reference. Some have used hydrogen-terminated single-crystal silicon (Si) because its surface is said to be stable, consisting of no native oxides. However, this stability lasts for only several tens of minutes<sup>4</sup> after which this sample can no longer be considered a reliable reference material.

In this paper we propose a novel technique for obtaining reliable ellipsometric measurements based on the use of twin photons produced by the process of spontaneous optical parametric downconversion (SPDC).<sup>9–14</sup> This source has been used effectively in many applications. We extend the use of this non-classical light source to the field of ellipsometry,<sup>15,16</sup> and demonstrate that absolute ellipsometric results can be obtained from a sample.

## 2. ELLIPSOMETRY USING TWIN-PHOTONS

All classical optical sources (including ideal amplitude-stabilized lasers) suffer from unavoidable quantum fluctuations even if all other extraneous noise sources are removed. Fluctuations in the photon number can only be eliminated by constructing a source that emits non-overlapping wave packets, each of which contains a fixed photon number. Such sources have been investigated, and indeed sub-Poisson light sources have been demonstrated.<sup>17–19</sup>

One such source may be readily realized via the process of spontaneous parametric downconversion (SPDC) from a second-order nonlinear crystal (NLC) when illuminated with a monochromatic laser beam (pump).<sup>13</sup> A portion of the pump photons disintegrate into photon pairs. The two photons that comprise the pair, known as signal and idler, are highly correlated since they conserve the energy (frequency-matching) and momentum (phase-matching) of the parent pump photon.

In type-II SPDC the signal and idler photons have orthogonal polarizations, one extraordinary and the other ordinary. These two photons emerge from the NLC with a relative time delay due to the birefringence of the NLC.<sup>20</sup> Passing the pair through an appropriate birefringent material of suitable length compensates for this time delay. This temporal compensation is required for extracting  $\psi$  and  $\Delta$  from the measurements; it is shown subsequently that when compensation is not employed one may obtain  $\psi$  but not  $\Delta$ .

The signal and idler may be emitted in two different directions, a case known as non-collinear SPDC, or in the same direction, a case known as collinear SPDC. In the former situation, the SPDC state is polarization entangled; its quantum state is described by<sup>20</sup>

$$|\Psi\rangle = \frac{1}{\sqrt{2}}(|HV\rangle + |VH\rangle), \quad (1)$$

where  $H$  and  $V$  represent horizontal and vertical polarizations, respectively.<sup>21</sup> It is understood that the first polarization indicated in a ket is that of the signal photon and the second is that of the idler. Such a state may not be written as the product of states of the signal and idler photons. Although Eq. (1) represents a pure quantum state, the signal and idler photons considered separately are each unpolarized.<sup>22,23</sup> The state represented in Eq. (1) assumes that there is no relative phase between the two kets. Although the relative phase may not be zero, it can, in general, be arbitrarily chosen by making small adjustments to the NLC.

In the collinear case the SPDC state is in a polarization-product state

$$|\Psi\rangle = |HV\rangle. \quad (2)$$

Because this state is factorizable (i.e., it may be written as the product of states of the signal and idler photons), it is not entangled.

A configuration based on the use of non-collinear type-II SPDC will be discussed. Such a setup, referred to as the *entangled twin-photon ellipsometer*,<sup>15,16</sup> or quantum ellipsometer, makes use of polarization-entangled photon pairs. This arrangement will be described using a generalization of the Jones-matrix formalism appropriate for twin-photon polarized beams.

## 2.1. Quantum Ellipsometry Using Polarization-Entangled Twin Photons

In this section it will be shown that one can construct an interferometer that makes use of quantum entanglement without the use of a beam splitter. This has the salutary effect of keeping 100% of the incoming photon flux (rather than 50%) while eliminating the requirement of characterizing it. Moreover, no other optical elements are introduced, so one need not be concerned with the characterization of any components. This is a remarkable feature of entanglement-based quantum interferometry.

The NLC is adjusted to produce SPDC in a type-II non-collinear configuration, as illustrated in Fig. 2. A matrix formalism that facilitates the derivation of the fields at the detectors is introduced. We begin by defining a *twin-photon Jones vector* that represents the field operators of the signal and idler in two spatially distinct modes. If  $\hat{a}_s(\omega)$  and  $\hat{a}_i(\omega')$  are the boson annihilation operators for the signal-frequency mode  $\omega$  and idler-frequency mode  $\omega'$ , respectively, then the twin-photon Jones vector of the field immediately after the NLC is

$$\hat{\mathbf{J}}_1 = \begin{pmatrix} \hat{\mathbf{A}}_s(\omega) + \hat{\mathbf{A}}_i(\omega') \\ \hat{\mathbf{A}}_s(\omega) + \hat{\mathbf{A}}_i(\omega') \end{pmatrix}, \quad (3)$$

where  $\hat{\mathbf{A}}_s(\omega) = \hat{a}_s(\omega) \begin{pmatrix} 1 \\ 0 \end{pmatrix}$  and  $\hat{\mathbf{A}}_i(\omega') = \hat{a}_i(\omega') \begin{pmatrix} 0 \\ 1 \end{pmatrix}$ .<sup>24</sup> The vectors  $\begin{pmatrix} 1 \\ 0 \end{pmatrix}$  (horizontal) and  $\begin{pmatrix} 0 \\ 1 \end{pmatrix}$  (vertical) are the familiar Jones vectors representing orthogonal polarization states.<sup>25</sup> The operators  $\hat{\mathbf{A}}_s(\omega)$  and  $\hat{\mathbf{A}}_i(\omega')$  thus are annihilation operators that include the vectorial polarization information of the field mode. The first element in  $\hat{\mathbf{J}}_1$ ,  $\hat{\mathbf{A}}_s(\omega) + \hat{\mathbf{A}}_i(\omega')$  represents the annihilation operator of the field in beam 1, which is a superposition of signal and idler field operators, while the second element corresponds to the annihilation operator of the field in beam 2.

We now define a *twin-photon Jones matrix* that represents the action of linear deterministic optical elements, placed in the two beams, on the polarization of the field as follows:

$$\mathbf{T} = \begin{pmatrix} \mathbf{T}_{11} & \mathbf{T}_{12} \\ \mathbf{T}_{21} & \mathbf{T}_{22} \end{pmatrix}, \quad (4)$$

where  $\mathbf{T}_{kl}$  ( $k, l = 1, 2$ ) is the familiar  $2 \times 2$  Jones matrix that represents the polarization transformation performed by a linear deterministic optical element. The indices refer to the spatial modes of the input and output beams. For example,  $\mathbf{T}_{11}$  is the Jones matrix of an optical element placed in beam 1 whose output is also in beam 1, whereas  $\mathbf{T}_{21}$  is the Jones matrix of an optical element placed in beam 1 whose output is in beam 2, and similarly for  $\mathbf{T}_{12}$  and  $\mathbf{T}_{22}$ . The twin-photon Jones matrix  $\mathbf{T}$  transforms a twin-photon Jones vector  $\hat{\mathbf{J}}_1$  into  $\hat{\mathbf{J}}_2$  according to  $\hat{\mathbf{J}}_2 = \mathbf{T}\hat{\mathbf{J}}_1$ .

Applying this formalism to the arrangement in Fig. 2, assuming that beams 1 and 2 impinge on the two polarization analyzers  $A_1$  and  $A_2$  directly (in absence of the sample), the twin-photon Jones matrix is given by

$$\mathbf{T}_p = \begin{pmatrix} \mathbf{P}(-\theta_1) & \mathbf{0} \\ \mathbf{0} & \mathbf{P}(\theta_2) \end{pmatrix}, \quad (5)$$

where  $\mathbf{P}(\theta) = \begin{pmatrix} \cos^2 \theta & \cos \theta \sin \theta \\ \cos \theta \sin \theta & \sin^2 \theta \end{pmatrix}$ , and  $\theta_1$  and  $\theta_2$  are the angles of the axes of the analyzers with respect to the horizontal direction. In this case the twin-photon Jones vector following the analyzers is therefore

$$\hat{\mathbf{J}}_2 = \mathbf{T}_p \hat{\mathbf{J}}_1 = \begin{pmatrix} \mathbf{P}(-\theta_1) \{ \hat{\mathbf{A}}_s(\omega) + \hat{\mathbf{A}}_i(\omega') \} \\ \mathbf{P}(\theta_2) \{ \hat{\mathbf{A}}_s(\omega) + \hat{\mathbf{A}}_i(\omega') \} \end{pmatrix}$$

$$= \begin{pmatrix} \{\cos \theta_1 \hat{a}_s(\omega) + \sin \theta_1 \hat{a}_i(\omega')\} \begin{pmatrix} \cos \theta_1 \\ -\sin \theta_1 \end{pmatrix} \\ \{\cos \theta_2 \hat{a}_s(\omega) + \sin \theta_2 \hat{a}_i(\omega')\} \begin{pmatrix} \cos \theta_2 \\ \sin \theta_2 \end{pmatrix} \end{pmatrix}. \quad (6)$$

Using the twin-photon Jones vector  $\hat{\mathbf{J}}_2$  one can obtain expressions for the fields at the detectors. The positive-frequency components of the field at detectors D<sub>1</sub> and D<sub>2</sub>, denoted  $\hat{\mathbf{E}}_1^+$  and  $\hat{\mathbf{E}}_2^+$  respectively, are given by

$$\hat{\mathbf{E}}_1^+(t) = \{\cos \theta_1 \int d\omega e^{-j\omega t} \hat{a}_s(\omega) + \sin \theta_1 \int d\omega' e^{-j\omega' t} \hat{a}_i(\omega')\} \begin{pmatrix} \cos \theta_1 \\ -\sin \theta_1 \end{pmatrix}, \quad (7)$$

$$\hat{\mathbf{E}}_2^+(t) = \{\cos \theta_2 \int d\omega e^{-j\omega t} \hat{a}_s(\omega) + \sin \theta_2 \int d\omega' e^{-j\omega' t} \hat{a}_i(\omega')\} \begin{pmatrix} \cos \theta_2 \\ \sin \theta_2 \end{pmatrix}, \quad (8)$$

while the negative frequency components are given by their Hermitian conjugates. With these fields one can show that the coincidence rate  $N_c \propto \sin^2(\theta_1 + \theta_2)$ .<sup>16</sup>

Consider now that the sample, assumed to have frequency-independent reflection coefficients, is placed in the optical arrangement illustrated in Fig. 2, and that the polarizations of the downconverted photons are along the eigenpolarizations of the sample. The effect of the sample, placed in beam 1, may be represented by the following twin-photon Jones matrix

$$\mathbf{T}_s = \begin{pmatrix} \mathbf{R} & \mathbf{0} \\ \mathbf{0} & \mathbf{I} \end{pmatrix}, \quad (9)$$

where

$$\mathbf{R} = \begin{pmatrix} \tilde{r}_1 & 0 \\ 0 & \tilde{r}_2 \end{pmatrix}, \quad (10)$$

$\mathbf{I}$  is the 2×2 identity matrix, and  $\tilde{r}_1$  and  $\tilde{r}_2$  are the complex reflection coefficients of the sample described earlier. The twin-photon Jones vector after reflection from the sample and passage through the polarization analyzers is given by

$$\hat{\mathbf{J}}_3 = \mathbf{T}_p \mathbf{T}_s \hat{\mathbf{J}}_1 = \begin{pmatrix} \{\tilde{r}_1 \cos \theta_1 \hat{a}_s(\omega) + \tilde{r}_2 \sin \theta_1 \hat{a}_i(\omega')\} \begin{pmatrix} \cos \theta_1 \\ -\sin \theta_1 \end{pmatrix} \\ \{\cos \theta_2 \hat{a}_s(\omega) + \sin \theta_2 \hat{a}_i(\omega')\} \begin{pmatrix} \cos \theta_2 \\ \sin \theta_2 \end{pmatrix} \end{pmatrix}, \quad (11)$$

which results in

$$\hat{\mathbf{E}}_1^+(t) = \{\tilde{r}_1 \cos \theta_1 \int d\omega e^{-j\omega t} \hat{a}_s(\omega) + \tilde{r}_2 \sin \theta_1 \int d\omega' e^{-j\omega' t} \hat{a}_i(\omega')\} \begin{pmatrix} \cos \theta_1 \\ -\sin \theta_1 \end{pmatrix}, \quad (12)$$

with  $\hat{\mathbf{E}}_2^+(t)$  identical to Eq. (8), since there is no sample in this beam.

Finally, it is straightforward to show that

$$N_c = C [\tan \psi \cos^2 \theta_1 \sin^2 \theta_2 + \sin^2 \theta_1 \cos^2 \theta_2 + 2\sqrt{\tan \psi} \cos \Delta \cos \theta_1 \cos \theta_2 \sin \theta_1 \sin \theta_2], \quad (13)$$

where the constant of proportionality  $C$  depends on the efficiencies of the detectors and the duration of accumulation of coincidences.<sup>16</sup> One can obtain  $C$ ,  $\psi$ , and  $\Delta$  by setting, for example,  $\theta_1 = 0^\circ$ ,  $\theta_1 = 90^\circ$ , and  $\theta_1 = 45^\circ$ , while  $\theta_2$  is scanned at each setting of  $\theta_1$ .

If the sample is replaced by a *perfect* mirror, the coincidence rate in Eq. (13) becomes a sinusoidal pattern of 100% visibility,  $C \sin^2(\theta_1 + \theta_2)$ , as previously indicated. In practice, by judicious control of the apertures placed in the down-converted beams, visibilities close to 100% can be obtained.

To understand the need for temporal compensation discussed previously, we re-derive Eq. (13), which assumes full compensation, when a birefringent compensator is placed in one of the arms of the configuration:

$$N_c = C[\tan \psi \cos^2 \theta_1 \sin^2 \theta_2 + \sin^2 \theta_1 \cos^2 \theta_2 + 2\sqrt{\tan \psi} \cos \Delta \cos \theta_1 \cos \theta_2 \sin \theta_1 \sin \theta_2 \Phi(\tau) \cos(\omega_o \tau)]. \quad (14)$$

Here  $\tau$  is the birefringent delay,  $\omega_o$  is half the pump frequency, and  $\Phi(\tau)$  is the Fourier transform of the SPDC normalized power spectrum. When  $\tau = 0$  we recover Eq. (13), whereas when  $\tau$  is larger than the inverse of the SPDC bandwidth, the third term that includes  $\Delta$  becomes zero and thus  $\Delta$  cannot be determined.

An interesting feature of this interferometer is that it is not sensitive to an overall mismatch in the length of the two arms of the setup and this increases the robustness of the arrangement. An advantage of this setup over

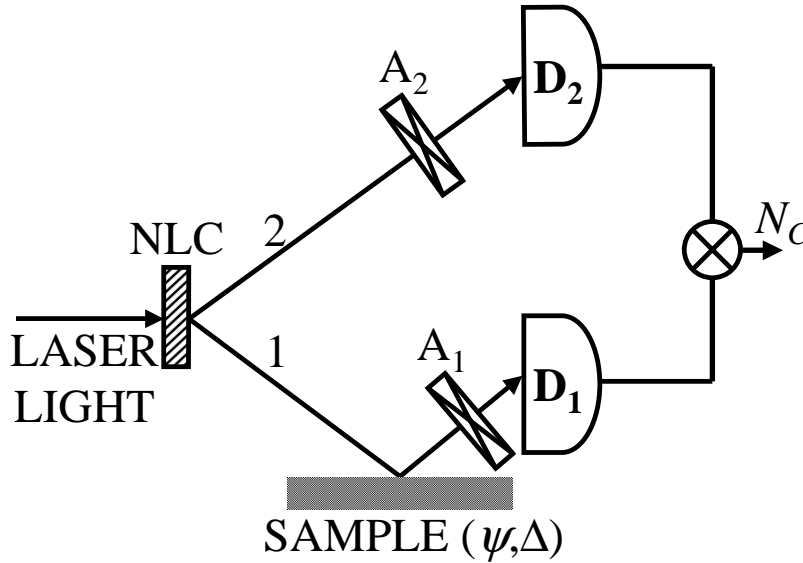


**Figure 2.** Polarization-entangled twin-photon ellipsometer.

its idealized null ellipsometric counterpart, discussed earlier, is that the two arms of the ellipsometer are separate and the light beams traverse them independently in different directions. This allows various instrumentation errors of the classical setup to be circumvented. For example, placing optical elements before the sample causes beam deviation errors<sup>26</sup> when the faces of the optical components are not exactly parallel. This leads to an error in the angle of incidence and, consequently, errors in the estimated parameters. In our case no optical components are placed between the source (NLC) and the sample; any desired polarization manipulation may be performed in the other arm of the entangled twin-photon ellipsometer. Furthermore, one can change the angle of incidence to the sample easily and repeatedly.

A significant drawback of classical ellipsometry is the difficulty of fully controlling the polarization of the incoming light. A linear polarizer is usually employed at the input of the ellipsometer, but the finite extinction coefficient of this polarizer causes errors in the estimated parameters.<sup>3</sup> In the entangled twin-photon ellipsometer the polarization of the incoming light is dictated by the phase-matching conditions of the nonlinear interaction in the NLC. The polarizations defined by the orientation of the optical axis of the NLC play the role of the input polarization in classical ellipsometry. The NLC is aligned for type-II SPDC so that only one polarization component of the pump generates SPDC, whereas the orthogonal (undesired) component of the

pump does not (since it does not satisfy the phase-matching conditions). The advantage is therefore that the downconversion process assures the stability of polarization along a particular direction.

## 2.2. Experimental Results

Preliminary experiments have shown that polarization-entangled photon pairs can be used to obtain values of  $\psi$  that are comparable to those obtained from traditional ellipsometers.

Using the setup shown in Fig. 2, a Si sample was tested at an angle of incidence of  $30^\circ$ . A 406-nm cw Kr<sup>+</sup> laser pump illuminated a beta-barium borate NLC to produce degenerate twin photons centered at 812 nm. Two avalanche photodiodes operating in the Geiger mode were used as detectors (D<sub>1</sub> and D<sub>2</sub>). Interference filters centered at 810 nm with 10-nm bandwidths were placed in front of each detector.

In the initial procedure, the angle of the analyzer A<sub>1</sub>, denoted  $\theta_1$ , was set to  $90^\circ$  while  $\theta_2$  was scanned. The sinusoidal pattern for the coincidence rate at this setting is shown in Fig. 3. Referring to Eq. (13), which, for  $\theta_1=90^\circ$ , reduces to

$$N_c = C \cos^2 \theta_2 \quad (15)$$

reveals that the amplitude of this curve provides the value for  $C$ .

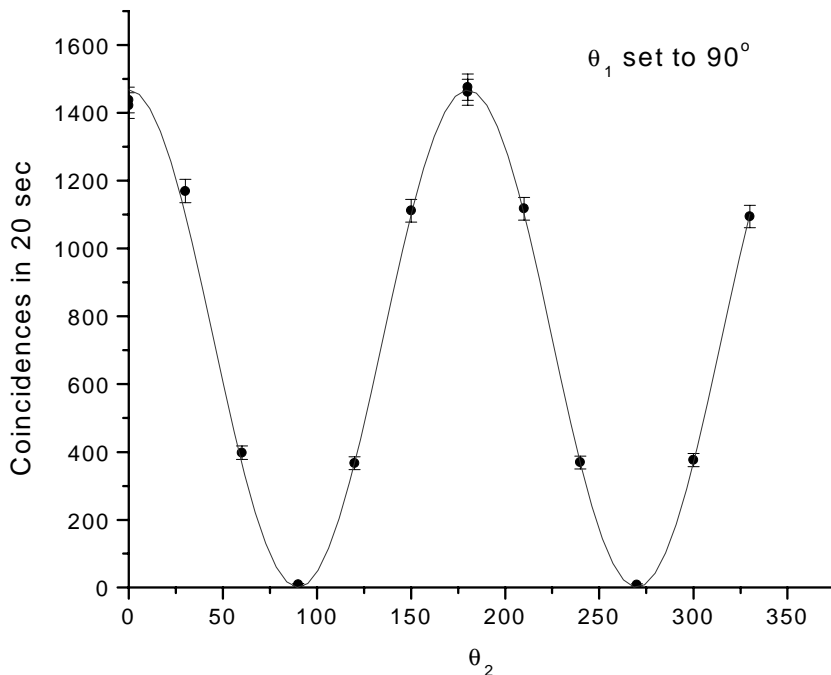


**Figure 3.** Coincidence interference pattern determined by scanning the angle  $\theta_2$ , with  $\theta_1$  fixed at  $90^\circ$ .

In the second part of the procedure,  $\theta_1$  was set to  $0^\circ$  while  $\theta_2$  was again scanned. The results for the coincidences are shown in Fig. 4. In this case Eq. (13) reduces to

$$N_c = C[\tan \psi \sin^2 \theta_2], \quad (16)$$

so that the amplitude of this function is equal to  $C \tan \psi$ . One can therefore determine  $\psi$  simply by dividing the two functions. Using this approach,  $\psi$  was determined to be  $40.2^\circ$  for our Si sample. The expected value for

$\psi$  at this angle of incidence is  $40.4^\circ$  in accordance with calculations carried out using the appropriate Sellmeier dispersion formula.<sup>27, 28</sup>

Unfortunately, the interference patterns obtained using a technique similar to the one described above did not provide a reasonable value for  $\Delta$ . The main reason for this comes from the fact that the equations used to obtain  $\psi$  assumed a visibility of 100%. In order to obtain  $\Delta$ , Eq. (13) must be re-written to include a visibility term that can assume a value less than 100%.

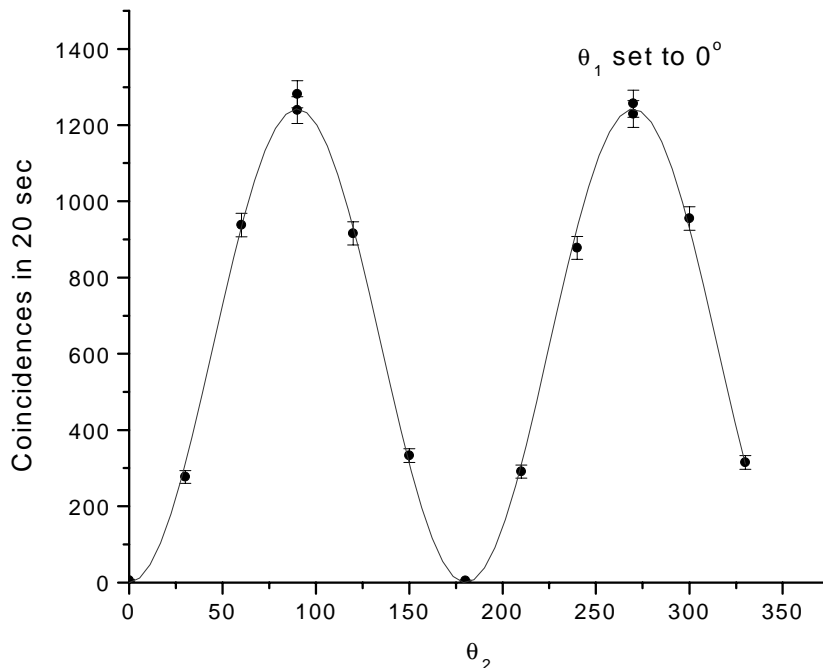


**Figure 4.** Coincidence interference pattern determined by scanning the angle  $\theta_2$ , with  $\theta_1$  fixed at  $0^\circ$ .

Another potential source of error resides in the model used to determine the ellipsometric parameters. It is well known that, unless specially treated, semiconductors become oxidized by air, thus, developing thin oxide layers. Therefore, the sample model should account for this thin oxide layer by considering a three-phase, rather than a two-phase, system. Either model would lead to a significantly different  $\Delta$  for the same sample.

### 2.3. Conclusion

Classical ellipsometric measurements are limited in their accuracy by virtue of the need for an absolutely calibrated source and detector. Mitigating this limitation requires the use of a well-characterized reference sample in a null configuration.

Preliminary experimental results for  $\psi$  for a silicon sample have been reported. We have demonstrated that entangled twin-photon ellipsometry is self-referencing and therefore eliminates the necessity of constructing an interferometer altogether. The underlying physics that leads to this remarkable result is the presence of fourth-order (coincidence) quantum interference of the photon pairs in conjunction with nonlocal polarization entanglement.

Our quantum ellipsometer is subject to the same shot-noise-limited, as well as angularly resolved, *precision* that is obtained with traditional ellipsometers (interferometric and null systems, respectively), but removes the limitation in *accuracy* that results from the necessity of using a reference sample in traditional ellipsometers.

Since the SPDC source is inherently broadband, narrowband spectral filters must be used to ensure that the ellipsometric data are measured at a specific frequency. Spectroscopic data can be obtained by employing a bank of such filters. Alternatively, techniques from Fourier-transform spectroscopy may be used to directly make use of the broadband nature of the source in ellipsometric measurements.

## REFERENCES

1. J. Vanhellefont, H. E. Maes, M. Schaekers, A. Armigliato, H. Cerva, A. Cullis, J. de Sande, H. Dinges, J. Hallais, V. Nayar, C. Pickering, J.-L. Stehlé, J. V. Landuyt, C. Walker, H. Werner, and P. Salieri, "Round robin investigation of silicon oxide on silicon reference materials for ellipsometry," *Appl. Surf. Sci.* **63**, pp. 45–51, 1993.
2. P. Drude, "Bestimmung optischer Konstanten der Metalle," *Ann. d. Physik u. Chemie* **39**, pp. 481–554, 1890.
3. R. M. A. Azzam and N. M. Bashara, *Ellipsometry and Polarized Light*, North-Holland, Amsterdam, 1977.
4. H. G. Tompkins and W. A. McGahan, *Spectroscopic Ellipsometry and Reflectometry*, Wiley, New York, 1999.
5. A. Rothen, "The ellipsometer, an apparatus to measure thicknesses of thin surface films," *Rev. Sci. Instrum.* **16**, pp. 26–30, 1945.
6. A. B. Winterbottom, "Optical methods of studying films on reflecting bases depending on polarization and interference phenomena," *Trans. Faraday Society* **42**, pp. 487–495, 1946.
7. M. Mansuripur, "Ellipsometry," *Opt. & Phot. News* **11** (4), pp. 52–56, 2000.
8. S. C. Russev, J. Drolet, and D. Ducharme, "Standards for which the ellipsometric parameter  $\psi$  remains insensitive to variations in the angle of incidence," *Appl. Opt.* **37**, pp. 5912–5922, 1998.
9. D. N. Klyshko, "Coherent decay of photons in a nonlinear medium," *Pis'ma Zh. Eksp. Teor. Fiz.* **6**, pp. 490–492, 1967. [Sov. Phys. JETP Lett. 6, 23-25 (1967)].
10. S. E. Harris, M. K. Oshman, and R. L. Byer, "Observation of tunable optical parametric fluorescence," *Phys. Rev. Lett.* **18**, pp. 732–735, 1967.
11. T. G. Giallorenzi and C. L. Tang, "Quantum theory of spontaneous parametric scattering of intense light," *Phys. Rev.* **166**, pp. 225–233, 1968.
12. D. A. Kleinman, "Theory of optical parametric noise," *Phys. Rev.* **174**, pp. 1027–1041, 1968.
13. D. N. Klyshko, *Photons and Nonlinear Optics*, ch. 1 and 6. Nauka, Moscow, 1980. [Translation: Gordon and Breach, 1988].
14. M. Atatüre, G. DiGiuseppe, M. D. Shaw, A. V. Sergienko, B. E. A. Saleh, and M. C. Teich, "Multiparameter entanglement in quantum interferometry," *Phys. Rev. A*, 2002. To be published.
15. A. F. Abouraddy, K. C. Toussaint, Jr., A. V. Sergienko, B. E. A. Saleh, and M. C. Teich, "Ellipsometric measurements by use of photon pairs generated by spontaneous parametric down-conversion," *Opt. Lett.* **26**, pp. 1717–1719, 2001.
16. A. F. Abouraddy, K. C. Toussaint, Jr., A. V. Sergienko, B. E. A. Saleh, and M. C. Teich, "Entangled-photon ellipsometry," *J. Opt. Soc. Am. B* **19**, pp. 656–662, 2002. Note that in Eqs. 13 – 15,  $\tan^2 \psi$  should be replaced by  $\tan \psi$ , and  $\tan \psi$  should be replaced by  $\sqrt{\tan \psi}$ .
17. M. C. Teich and B. E. A. Saleh, "Observation of sub-Poisson Franck-Hertz light at 253.7 nm," *J. Opt. Soc. Am. B* **2**, pp. 275–282, 1985.
18. M. C. Teich and B. E. A. Saleh, "Photon bunching and antibunching," *Progress in Optics* **26**, pp. 1–104, 1988.
19. M. C. Teich and B. E. A. Saleh, "Squeezed and antibunched light," *Physics Today* **43**(6), pp. 26–34, 1990.
20. P. G. Kwiat, K. Mattle, H. Weinfurter, A. Zeilinger, A. V. Sergienko, and Y. H. Shih, "New high-intensity source of polarization-entangled photon pairs," *Phys. Rev. Lett.* **75**, pp. 4337–4341, 1995.
21. A. V. Sergienko, Y. H. Shih, and M. H. Rubin, "Experimental evaluation of a two-photon wave packet in type-(II) optical parametric downconversion," *J. Opt. Soc. Am. B* **12**, pp. 859–862, 1995.
22. U. Fano, "Description of states in quantum mechanics by density matrix and operator techniques," *Rev. Mod. Phys.* **29**, pp. 74–93, 1957.

23. A. F. Abouraddy, B. E. A. Saleh, A. V. Sergienko, and M. C. Teich, "Degree of entanglement for two qubits," *Phys. Rev. A* **64**, p. 050101(R), 2001.
24. R. J. Glauber, "Optical coherence and photon statistics," in *Quantum Optics and Electronics*, C. DeWitt, A. Blandin, and C. Cohen-Tannoudji, eds., pp. 63–185, Gordon and Breach, New York, 1965. Lectures delivered at Les Houches 1964 summer school.
25. B. E. A. Saleh and M. C. Teich, *Fundamentals of Photonics*, Wiley, New York, 1991.
26. J. R. Zeidler, R. B. Kohles, and N. M. Bashara, "Beam deviation errors in ellipsometric measurements; an analysis," *Appl. Opt.* **13**, pp. 1938–1945, 1974.
27. E. D. Palik, ed., *Handbook of Optical Constants of Solids*, Academic Press, New York, 1985.
28. E. D. Palik, ed., *Handbook of Optical Constants of Solids III*, Academic Press, New York, 1995.